

*Equation of state of a synthetic ulvöspinel,
(Fe_{1.94}Ti_{0.03})Ti_{1.00}O_{4.00}, at ambient
temperature*

**Zhihua Xiong, Xi Liu, Sean R. Shieh,
Fei Wang, Xiang Wu, Xinguo Hong &
Yonghong Shi**

Physics and Chemistry of Minerals

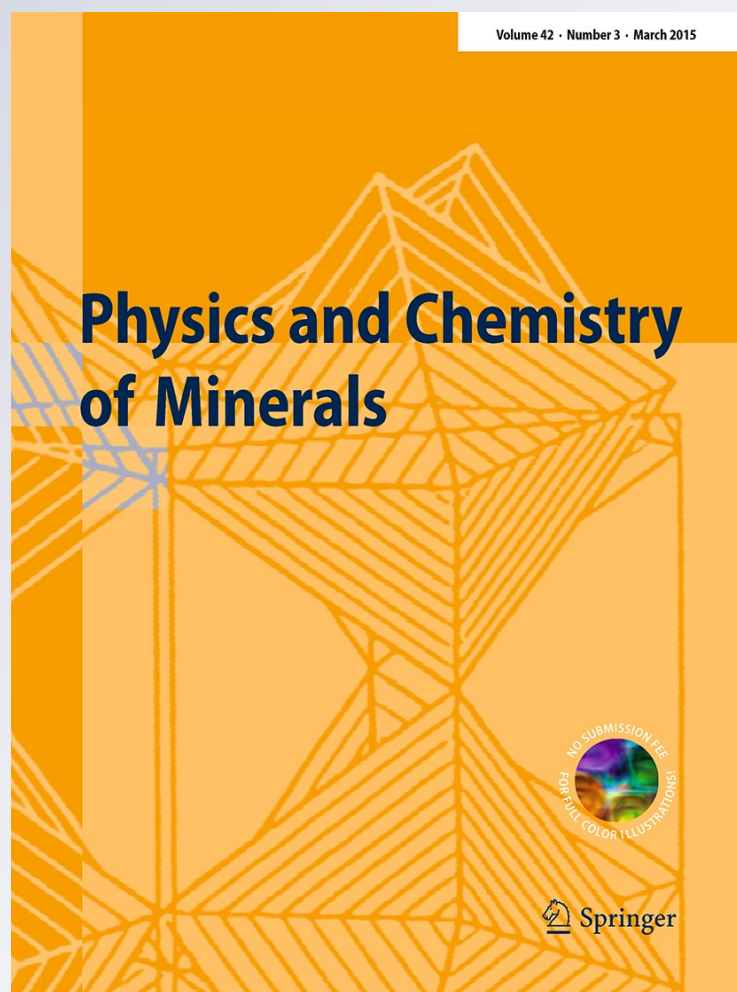
ISSN 0342-1791

Volume 42

Number 3

Phys Chem Minerals (2015) 42:171-177

DOI 10.1007/s00269-014-0704-y



Your article is protected by copyright and all rights are held exclusively by Springer-Verlag Berlin Heidelberg. This e-offprint is for personal use only and shall not be self-archived in electronic repositories. If you wish to self-archive your article, please use the accepted manuscript version for posting on your own website. You may further deposit the accepted manuscript version in any repository, provided it is only made publicly available 12 months after official publication or later and provided acknowledgement is given to the original source of publication and a link is inserted to the published article on Springer's website. The link must be accompanied by the following text: "The final publication is available at link.springer.com".

Equation of state of a synthetic ulvöspinel, $(\text{Fe}_{1.94}\text{Ti}_{0.03})\text{Ti}_{1.00}\text{O}_{4.00}$, at ambient temperature

Zhihua Xiong · Xi Liu · Sean R. Shieh · Fei Wang ·
Xiang Wu · Xinguo Hong · Yonghong Shi

Received: 9 April 2014 / Accepted: 15 August 2014 / Published online: 27 August 2014
© Springer-Verlag Berlin Heidelberg 2014

Abstract Using a diamond-anvil cell and synchrotron X-ray diffraction, the compressional behavior of a synthetic ulvöspinel $(\text{Fe}_{1.94}\text{Ti}_{0.03})\text{Ti}_{1.00}\text{O}_{4.00}$ has been investigated up to about 7.05 GPa at 300 K. The pressure–volume data fitted to the second-order Birch–Murnaghan equation of state yield an isothermal bulk modulus (K_T) of 147(4) GPa (K'_T fixed as 4). This value is slightly larger than that previously determined by an ultrasonic pulse echo method (121(2) GPa; Syono et al., *J Phys Soc Jpn* 31:471–476, 1971), but substantially smaller than that recently determined by a synchrotron X-ray diffraction technique (251(3) GPa; Yamanaka et al., *Phys Rev B* 80:134120, 2009; *Am Mineral* 98:736–744, 2013). Combined with the K_T of magnetite (Fe_3O_4 ; ~182(3) GPa), our finding suggests that the bulk modulus of the solid solutions $\text{Fe}_{3-x}\text{Ti}_x\text{O}_4$ ($0 \leq x \leq 1$) along the join magnetite–ulvöspinel decreases by ~20 %.

Keywords Compressibility · Diamond-anvil cell · Synchrotron X-ray diffraction · Ulvöspinel

Introduction

Natural ulvöspinel is a common accessory mineral in terrestrial metamorphic and igneous rocks, and is an abundant phase in the high Ti environment of the lunar crust (Cameron 1971). With small amounts of additional Mg_2TiO_4 and Mn_2TiO_4 , its compositions mainly fall along the join magnetite (Fe_3O_4)–ulvöspinel (Fe_2TiO_4). The solid solutions along this join, known as titanomagnetites and with the spinel structure, are important minerals not only because of their applications as geothermometer and oxygen fugacity indicator (Buddington and Lindsley 1964; Spencer and Lindsley 1981; Andersen and Lindsley 1988), but also because of their contributions in the magnetic signals of many rocks such as the mid-ocean ridge basalts. Therefore, many experimental studies were conducted to investigate the physical and chemical properties of the titanomagnetites (e.g., Ishikawa et al. 1971; O'Neill et al. 1988; Bosi et al. 2008; Kyono et al. 2011; Lilova et al. 2012; Diego Gatta et al. 2014).

Compared to the numerous experimental investigations on the bulk modulus of magnetite (e.g., Haavik et al. 2000; Reichmann and Jacobsen 2004; Diego Gatta et al. 2007; Rozenberg et al. 2007; Yamanaka et al. 2013), the number of studies on the bulk modulus of ulvöspinel has been very limited. Further, the results obtained in these studies are currently in sharp discrepancy. Syono et al. (1971) pioneered in measuring the bulk modulus of ulvöspinel. By conducting ultrasonic pulse echo measurements on a single crystal of ulvöspinel, they obtained an adiabatic bulk modulus (K_S) as 121 GPa, with an error of about 2 GPa

Z. Xiong · X. Liu (✉) · F. Wang · X. Wu
Key Laboratory of Orogenic Belts and Crustal Evolution, MOE,
Peking University, Beijing 100871, People's Republic of China
e-mail: xi.liu@pku.edu.cn

Z. Xiong · X. Liu · F. Wang · X. Wu
School of Earth and Space Sciences, Peking University,
Beijing 100871, People's Republic of China

S. R. Shieh
Department of Earth Sciences, University of Western Ontario,
London, ON N6A 5B7, Canada

X. Hong
Mineral Physics Institute, State University of New York,
Stony Brook, NY 11974, USA

Y. Shi
School of Resource and Environment Engineering,
Hefei University of Technology, Hefei 230009,
People's Republic of China

(Liebermann et al. 1977). Recently, Yamanaka et al. (2009, 2013) carried out compression experiments up to ~ 9 GPa on both ulvöspinel single crystal (pressure medium: ethanol–methanol–water mixture; P measurement method: ruby fluorescence method; sample size: $60 \times 60 \times 20 \mu\text{m}^3$) and ulvöspinel powder (pressure medium: neon; P measurement method: ruby fluorescence method; gasket material: rhenium) with a diamond-anvil cell (DAC) and synchrotron X-ray diffraction. Their obtained value for the isothermal bulk modulus (K_T) of ulvöspinel was $\sim 251(3)$ GPa (the first pressure derivative of the isothermal bulk modulus, K'_T , fixed as 4). In principle, K_S and K_T are related by the equation $K_S = K_T (1 + \alpha\gamma T)$, where α is the volumetric thermal expansion coefficient and γ is the Grüneisen parameter. Since the value of the α of the spinels is usually in the range of $1\text{--}3 \times 10^{-5} \text{ K}^{-1}$ (Fei 1995; Wang et al. 2012) and that of the γ is commonly less than 2 (e.g., Chopelas and Hofmeister 1991; Hofmeister and Mao 2001; Wang et al. 2002, 2003; Yong et al. 2012), the difference between the K_S and K_T at ambient P – T condition, with K_S larger than K_T , is expected to be less than 10 GPa.

In this paper, we have investigated the equation of state of a synthetic ulvöspinel at ambient temperature using a diamond-anvil cell, coupled with synchrotron X-ray radiation. Subsequently, the obtained equation of state of ulvöspinel is compared to that of magnetite, to illustrate the variation pattern of the bulk modulus along the join Fe_3O_4 – Fe_2TiO_4 .

Experimental method

The ulvöspinel was synthesized in an open Pt capsule at 1,573 K for 24 h with a controlled oxygen fugacity of $f_{\text{O}_2} = 10^{-11}$. The product was once examined with electron microprobe analysis (EMPA; JEOL JXA-8200) and X-ray diffraction, and its high-pressure phase transition was investigated using X-ray diffraction and Mössbauer spectroscopy up to about 24 GPa (Wu et al. 2012). In this study, we further characterized this material using scanning electron microscope (SEM; FEI Quanta 650 FEG), EMPA (JEOL JXA-8230) and synchrotron X-ray diffraction.

The high-pressure angle dispersive X-ray diffraction experiments with a symmetrical DAC were conducted at the beamline X17C, National Synchrotron Light Source, Brookhaven National Laboratory. The experimental techniques were generally identical to those used in our previous studies (Liu et al. 2008, 2009; Fleet et al. 2010). Briefly, a T301 stainless steel plate was used as the gasket, a 4:1 methanol–ethanol mixture was used as the pressure medium, and a couple of ruby chips were used as the pressure marker (the ruby fluorescence method; Mao et al. 1978). The incident synchrotron radiation beam was

monochromatized to a wavelength of 0.4112 \AA , and its beam size was collimated to $\sim 25 \times 20 \mu\text{m}^2$. Each X-ray diffraction pattern at certain pressure was collected for about 10 min using an online CCD detector, and subsequently integrated to derive the conventional one-dimensional profile using the Fit2D program (Hammersley 1996). With a full profile refinement of the XRD data using the MDI's program Jade 5.0 (Material Data, Inc.), the positions of the diffraction peaks 111, 220, 311, 222, 400, 422, 511 and 440 were determined and later used to derive the unit-cell parameters of the ulvöspinel at different pressures. These data-processing techniques were used in our previous investigations (He et al. 2012; Chang et al. 2013).

Results and discussion

Electron back-scatter images obtained with the SEM show that the synthetic product from our high-temperature experiment at 1 atm (grain size ranging from 20 to 200 μm), used as the starting material in our high-pressure compression experiments, consists of one crystalline phase only (plus a trace amount of a melt-like compound). The XRD data identified this crystalline phase as ulvöspinel, but demonstrated another crystalline phase, a very small fraction of impurity ilmenite, at the same time. We took the advantage of this ilmenite impurity and used it as an internal gauge for examining the accuracy of our result about the ulvöspinel, since previous studies gave out very similar values for the isothermal bulk modulus of ilmenite (Wechsler and Prewitt 1984; Tronche et al. 2010).

The EMPA data (10 analyses) suggest a chemical formula of $\text{Fe}_{1.940(8)}\text{Ti}_{1.030(4)}\text{O}_{4.000}$ (all iron assumed as Fe^{2+}) for the ulvöspinel. This phenomenon, with Ti in slight excess of 1 atom per formula unit, is in contrast to some previous observations made by Ôno et al. (1968; $\text{Fe}_{2.05}\text{Ti}_{0.95}\text{O}_{4.00}$) and Sedler et al. (1994; $\text{Fe}_{2.068}\text{Ti}_{0.932}\text{O}_{4.000}$). Without any site occupation information, we tentatively write the ulvöspinel formula as $(\text{Fe}_{1.94}\text{Ti}_{0.03})\text{Ti}_{1.00}\text{O}_{4.00}$, which leads to the cation substitution mechanism $2\text{Fe}^{2+} = \text{Ti}^{4+}$. It appears that a trace amount of Ti (cation vacancy as well) on the tetrahedral sites of the ulvöspinel is inevitable. The presence of some Ti on the tetrahedral sites is currently a controversial issue; Wechsler et al. (1984) and Yamanaka et al. (2013) argued that Ti only occurs on the octahedral sites, whereas Forster and Hall (1965) and Sedler et al. (1994) demonstrated small amounts of Ti (up to 18 %) occupying the tetrahedral sites. We assume in this study that the effect of this trace amount of Ti (cation vacancy as well) on the tetrahedral sites on the physical properties of the ulvöspinel is negligible.

According to Akimoto and Syono (1967), Fe_2TiO_4 ulvöspinel breaks down to $\text{FeO} + \text{FeTiO}_3$ at about 4 GPa and

Table 1 Unit-cell parameters of ulvöspinel and impurity ilmenite at high pressure (room T)

P (GPa)	Ulvöspinel		Ilmenite			
	a (Å)	V (Å ³)	a (Å)	c (Å)	V (Å ³)	c/a
Compression						
0.77(0) ^a	8.504(2) ^b	614.9(2)	–	–	–	–
0.78(1)	8.506(1)	615.5(1)	5.075(2)	14.047(2)	313.3(2)	2.768(1)
1.70(3)	8.485(2)	610.9(2)	5.073(14)	13.963(54)	311.2(21)	2.752(13)
2.71(3)	8.473(1)	608.3(1)	5.068(5)	13.950(11)	310.3(7)	2.753(3)
3.91(3)	8.451(2)	603.5(2)	5.057(7)	13.957(9)	309.1(9)	2.760(4)
4.63(3)	8.436(1)	600.3(1)	5.050(2)	13.904(5)	307.1(3)	2.753(2)
5.66(3)	8.420(1)	596.9(1)	5.042(8)	13.885(12)	305.7(11)	2.754(5)
6.44(3)	8.415(2)	595.9(3)	5.032(10)	13.865(26)	304.1(13)	2.755(7)
7.05(3)	8.404(2)	593.5(3)	5.034(6)	13.829(8)	303.5(7)	2.747(4)
Decompression						
5.25(25)	8.431(2)	599.2(2)	5.046(8)	13.922(14)	308.3(11)	2.759(5)
3.97(3)	8.449(2)	603.0(2)	5.048(5)	13.968(9)	308.3(6)	2.767(3)
2.23(3)	8.469(2)	607.4(2)	5.066(17)	13.967(38)	310.5(22)	2.757(12)
1.04(3)	8.497(3)	613.5(3)	5.076(4)	14.014(7)	312.7(5)	2.761(2)

^a Pressure determined by averaging the values measured before and after collection of synchrotron data

^b Numbers in parentheses representing one standard deviation

1,473 K, with a positive Clapeyron slope for the P – T locus of the decomposition reaction. At room temperature, it transforms into a tetragonal phase at ~ 7.12 – 8.76 GPa (Yamanaka et al. 2009; Wu et al. 2012; Yamanaka et al. 2013). It is thus clear that a completed P – T diagram for ulvöspinel is still not available. To avoid the cubic-to-tetragonal phase transition, consequently, we conducted our high-pressure experiments up to 7.05 GPa only (Table 1). In total, nine X-ray diffraction patterns were collected during compression, while four were collected during decompression. Typical X-ray diffraction patterns are shown in Fig. 1. No peak broadening can be observed, which verifies the efficiency of our pressure medium to maintain a hydrostatic pressure condition in our experiments (Klotz et al. 2009). In addition, the X-ray diffraction pattern obtained at the maximum experimental pressure of 7.05 GPa shows no peak-splitting for the 220 peak, suggesting that the polymorphic phase transition was not reached (Yamanaka et al. 2009; Wu et al. 2012).

Duplicated analyses using the synchrotron radiation at ambient pressure give out the unit-cell parameters of the synthetic ulvöspinel as $a_0 = 8.5274(14)$ Å and $V_0 = 620.09(18)$ Å³, and $a_0 = 8.5231(19)$ Å and $V_0 = 619.14(24)$ Å³, respectively. These values are smaller than most early measurements (from $a_0 = 8.50(1)$ Å to $a_0 = 8.538(3)$ Å, as summarized in Sedler et al. (1994)), but in good agreement with the most recent observations (Bosi et al. 2009; Yamanaka et al. 2013). Different compositions caused by different synthesizing conditions such as varying temperature, oxygen fugacity, and employment of a flux or not are presumably the primary sources for the fluctuation of the unit-cell parameters at ambient P – T condition. In addition, the obtained room- P unit-cell parameters for the ilmenite

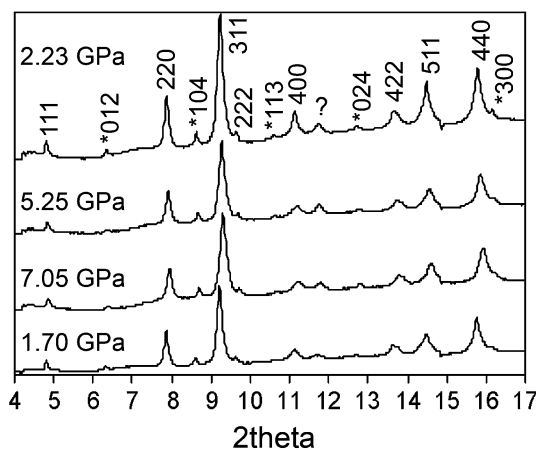


Fig. 1 Examples of X-ray diffraction patterns of ulvöspinel at 1.70, 7.05, 5.25 and 2.23 GPa. All major peaks can be assigned to ulvöspinel. Note that the weak diffraction peaks, denoted by the asterisks, are for the small amount of ilmenite impurity (ideally FeTiO₃). One unknown weak peak, denoted by a question marker, appears at about 11.7° (2θ)

impurity are: $a_0 = 5.087(5)$ Å, $c_0 = 14.055(17)$ Å and $V_0 = 315.03(77)$ Å³.

The effect of pressure on the unit-cell volume of the ulvöspinel is summarized in Table 1 and graphically shown in Fig. 2. A small non-linear dependence on pressure over the investigated pressure range has been observed for the unit-cell volume. Further, the volume data determined from the compression experiments and decompression experiments are well mixed, suggesting that the elastic behavior of ulvöspinel is fully reversible after compression to about 7 GPa. Compared to the data from Yamanaka et al. (2009;

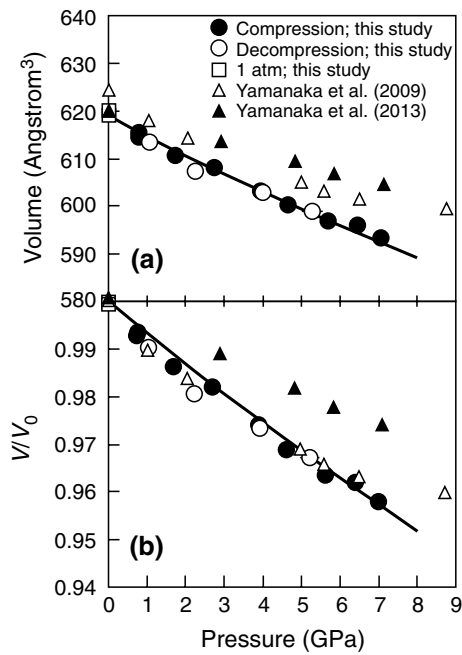


Fig. 2 Effect of pressure on the unit-cell parameters of ulvöspinel at 300 K, compared to those from Yamanaka et al. (2009, 2013): **a** the volume; **b** the V/V_0 ratio. *Thick curve* represents the second-order Birch–Murnaghan equation of state, established using all P – V data collected in this study. Note that for most data points, their *error bars* are approximate to or smaller than the symbols. V_0 and V represent the unit-cell volume at room pressure and high pressure, respectively

2013), Fig. 2a shows that the high-pressure volumes determined in this study are always smaller, with the difference between this study and Yamanaka et al. (2009; 2013) positively correlated with pressure. As to the pressure effect on the V/V_0 ratio (Fig. 2b), in contrast, most high-pressure data but the one at 8.76 GPa from Yamanaka et al. (2009) are in excellent agreement with our data, whereas all high-pressure data from Yamanaka et al. (2013) are not.

The effect of pressure on the unit-cell parameters of the ilmenite impurity is summarized in Table 1 and graphically shown in Fig. 3. Although the data are not as accurate as those for the ulvöspinel due to the low intensity of the X-ray diffraction peaks caused by the low-volume fraction of the ilmenite, concrete correlations between the unit-cell parameters and pressure have been well demonstrated, and good agreement between this study and Wechsler and Prewitt (1984) has been obtained.

To determine the elastic parameters, the P – V data have been fitted to the second-order Birch–Murnaghan equation of state (Birch 1947) by a least-squares method:

$$P = 3K_T f_E (1 + 2f_E)^{\frac{5}{2}}$$

where P is the pressure, K_T the isothermal bulk modulus, and f_E the Eulerian definition of finite strain, which is

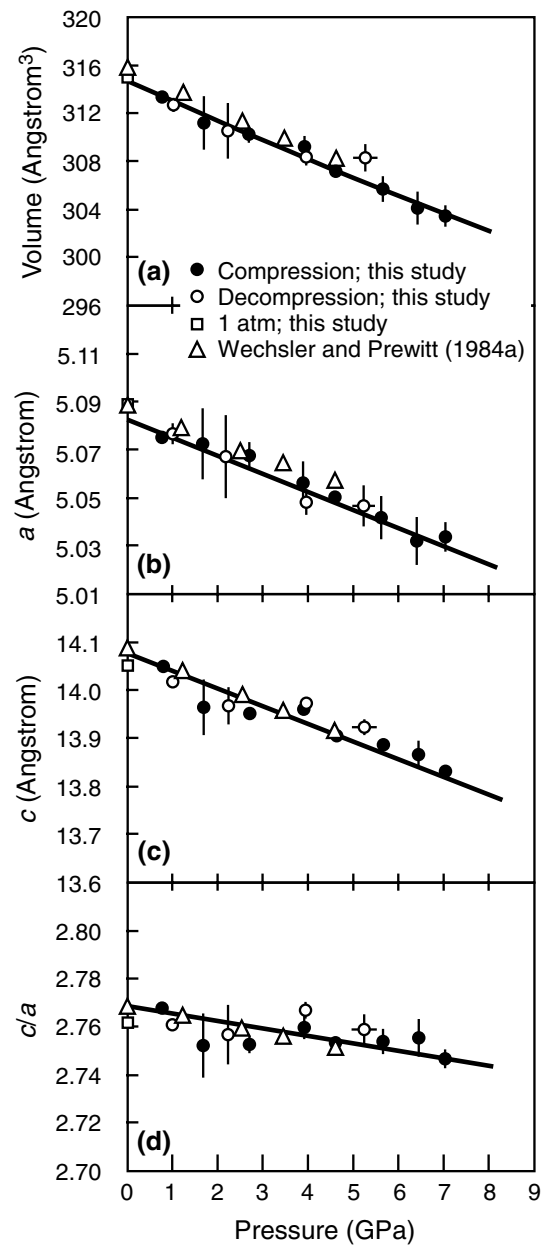


Fig. 3 Effect of pressure on the unit-cell parameters of ilmenite at 300 K, compared to those from Wechsler and Prewitt (1984). *Thick curve* represents the second-order Birch–Murnaghan equation of state, established using all P – V data collected in this study

$[(V_0/V)^{2/3} - 1]/2$, respectively. In the Eulerian definition of finite strain, V_0 is the volume at zero pressure, whereas V is the volume at high pressure. A fit with the third-order Birch–Murnaghan equation of state with variable K'_T has been tested, but generated unreasonable result due to the narrow pressure range of our experiments.

With K'_T fixed as 4, we have obtained (1) $K_T = 148(4)$ GPa and $V_0 = 618.91(36)$ Å³ with the ambient and compression data, (2) $K_T = 130(10)$ GPa and $V_0 = 619.50(70)$ Å³ with the ambient and decompression data, and (3)

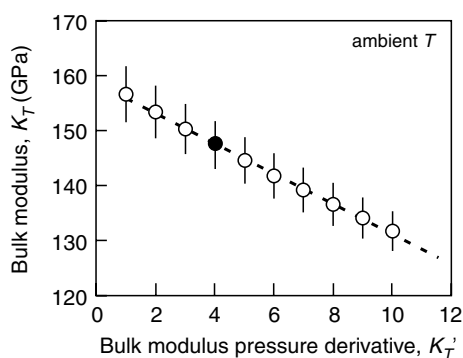


Fig. 4 Correlation of the isothermal bulk modulus of ulvöspinel and its first pressure derivative at ambient P and T

$K_T = 148(4)$ GPa and $V_0 = 618.78(37)$ Å³ with all data. We believe that $K_T = 148(4)$ GPa should be a good approximation to the real value of the isothermal bulk modulus of ulvöspinel. By fixing K'_T to different values and calculating K_T , a correlation analysis of K_T and K'_T has also been carried out, and the result is shown in Fig. 4. The value of the K_T decreases from 157(5) to 132(4) GPa as the K'_T value increases from 1 to 10.

Similarly, we have fitted all P – V data of the ilmenite impurity (Table 1), and obtained $K_T = 184(9)$ GPa and $V_0 = 314.66(22)$ Å³. This value for the K_T is in good agreement with Wechsler and Prewitt (1984; 177(3) GPa with K'_T assumed to be 4(1)), and Tronche et al. (2010; 181(7) with $K'_T = 3(1)$), suggesting that the data in this study have high quality. In addition, a linearized second-order Birch–Murnaghan equation of state (Angel 2000) was used to obtain the parameters of the equations of state for the crystallographic axes, yielding: $a_0 = 5.083(2)$ Å and $K_{T-a} = 219(19)$ GPa for the a -axis, and $c_0 = 14.076(5)$ Å and $K_{T-c} = 122(7)$ GPa for the c -axis. Therefore, ilmenite has a relatively strong elastic anisotropy, in good agreement with Wechsler and Prewitt (1984) as well.

The K_S of ulvöspinel was once determined as 121(2) GPa using an ultrasonic pulse echo method (Syono et al. 1971; Liebermann et al. 1977). Considering the accuracy of their experimental techniques in the 1970s, the result from Syono et al. (1971) is in good agreement with ours. If we assume for ulvöspinel at 1 atm and 298 K $\alpha = 2.06 \times 10^{-5}$ K⁻¹ (equal to that of magnetite; Fei 1995; Wang et al. 2012) and $\gamma = 2$ (a potentially maximum value), and adopt $K_T = 148$ GPa (this study), anyhow, the K_S value of ulvöspinel is predicted to be ~150 GPa, according to the equation $K_S = K_T(1 + \alpha\gamma T)$. It follows that a further experimental study on the K_S of ulvöspinel is desirable.

The K_T of ulvöspinel was recently constrained as 251(3) using a DAC + synchrotron X-ray radiation technique (Yamanaka et al. 2009, 2013). As shown in Fig. 2b, most experimental data from Yamanaka et al. (2009) are

Table 2 Isothermal bulk modulus of spinel solid solutions $\text{Fe}_{3-x}\text{Ti}_x\text{O}_4$ at ambient P and T

x	K_0	K'_T	Reference
0	217(2) ^a	4 ^b	Haavik et al. (2000)
0	186(3)	5.1(1)	Reichmann and Jacobsen (2004)
0	182(4)	3.6(8)	Diego Gatta et al. (2007)
0	180(1)	4 ^b	Diego Gatta et al. (2007)
0	181(1)	4.3(1)	Rozenberg et al. (2007)
0	220(5)	4 ^b	Yamanaka et al. (2013)
0.102	263(4)	4 ^b	Yamanaka et al. (2013)
0.231	269(5)	4 ^b	Yamanaka et al. (2013)
0.551	233(1)	4 ^b	Yamanaka et al. (2013)
0.624	275(6)	4 ^b	Yamanaka et al. (2013)
0.734	246(2)	4 ^b	Yamanaka et al. (2013)
0.831	242(2)	4 ^b	Yamanaka et al. (2013)
1	251(3)	4 ^b	Yamanaka et al. (2009, 2013)
1	121(2) ^c	–	Syono et al. (1971)
1	148(4)	4 ^b	This study

^a Numbers in parentheses representing one standard deviation

^b Fixed value

^c Adiabatic bulk modulus

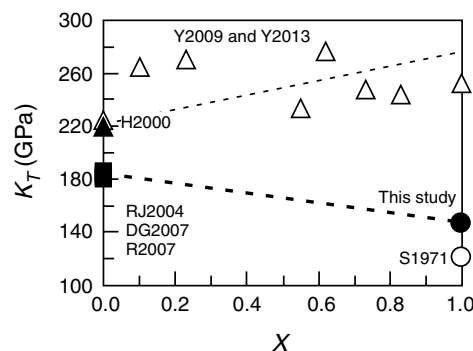


Fig. 5 Isothermal bulk moduli of solid solutions ($\text{Fe}_{3-x}\text{Ti}_x\text{O}_4$) along the join Fe_3O_4 – Fe_2TiO_4 at ambient P and T . Data for magnetite are from Haavik et al. (2000), Reichmann and Jacobsen (2004), Diego Gatta et al. (2007), Rozenberg et al. (2007) and Yamanaka et al. (2013), abbreviated as H2000, RJ2004, DG2007, R2007, and Y2013, respectively. Data for ulvöspinel are from Syono et al. (1971), Yamanaka et al. (2009, 2013) and this study, with Syono et al. (1971) and Yamanaka et al. (2009) abbreviated as S1971, and Y2009, respectively. Data for other compositions are from Yamanaka et al. (2013). The small difference between the K_S and K_T for the ulvöspinel is ignored

generally compatible with our data. The experiment at 8.76 GPa, displaying no sign of the cubic-to-tetragonal phase transition, was highly possibly subject to large pressure overestimation, as suggested by the experiment at 8.56 GPa in Yamanaka et al. (2013), which already demonstrated the phase transition. With the removal of the data at 8.76 GPa, the rest data from Yamanaka et al. (2009) constrain the K_T

of ulvöspinel as 152(8) GPa (uncertainty in the pressure measurements assumed as 0.01 GPa), a value in excellent agreement with our result. As to the much larger K_T estimated by Yamanaka et al. (2013), it is presently unclear what the real cause was. It is noted though that the ulvöspinel sample used by Yamanaka et al. (2013) is stoichiometric, whereas ours is $(\text{Fe}_{1.94}\text{Ti}_{0.03})\text{Ti}_{1.00}\text{O}_{4.00}$, with a trace amount of Ti and cation vacancy on the tetrahedral sites.

Recent experimental results about the isothermal bulk moduli of the solid solutions along the join Fe_3O_4 – Fe_2TiO_4 have been listed in Table 2 and graphically shown in Fig. 5. As summarized by Haavik et al. (2000), nine earlier independent studies constrained the K_T of magnetite, varying from 155 to 215 GPa. The recent experimental investigations (Haavik et al. 2000; Reichmann and Jacobsen 2004; Diego Gatta et al. 2007; Rozenberg et al. 2007; Yamanaka et al. 2013) have narrowed the variation range down to about 180–217 GPa. Haavik et al. (2000) obtained a slightly larger K_T for magnetite. They used N_2 as the pressure-transmitting medium and carried out high-pressure experiments up to about 30 GPa, so that their result might be affected by a nonhydrostatic experimental environment, as suggested by Klotz et al. (2009). Yamanaka et al. (2013) also obtained a slightly larger K_T for magnetite; their value was likely inaccurate, by the same token outlined in the preceding paragraph (the ulvöspinel case). Consequently, it seems appropriate to adopt a value of about 182(3) GPa as the K_T for magnetite (Reichmann and Jacobsen 2004; Diego Gatta et al. 2007; Rozenberg et al. 2007).

Figure 5 shows that along the join Fe_3O_4 – Fe_2TiO_4 , the K_T of the solid solutions $\text{Fe}_{3-x}\text{Ti}_x\text{O}_4$ ($0 \leq x \leq 1$) decreases from about 182(3) to 148(4) GPa, as x increases from 0 to 1. Accompanying this variation is an increase in the unit-cell volume, from about 591.8(3) Å³ (Reichmann and Jacobsen 2004; Diego Gatta et al. 2007; Rozenberg et al. 2007) to 618.78(37) Å³ (this study). The relative decrease in the bulk moduli along the join Fe_3O_4 – Fe_2TiO_4 is about 20 %, whereas the relative increase in the unit-cell volumes is about 4 % only.

It has been well established that the K_T is nearly inversely proportional to the specific volume for alkali halides, fluorides, selenides, sulfides, apatites, and 2–3 spinels (Anderson and Nafe 1965; Anderson and Anderson 1970; He et al. 2013). Our result obtained for ulvöspinel, combined with the result for magnetite, seems compatible with this relationship. On the contrary, the result from Yamanaka et al. (2013) does not (Fig. 5).

The exact contributor to the bulk modulus variations as shown in Fig. 5 is presently unclear. Both magnetite and ulvöspinel are generally inverse spinels (Fleet 1981; Wechsler et al. 1984), with their structural formula as $^{\text{T}}(\text{Fe}^{3+})^{\text{M}}(\text{Fe}^{2+}\text{Fe}^{3+})\text{O}_4$ and $^{\text{T}}(\text{Fe}^{2+})^{\text{M}}(\text{Fe}^{2+}\text{Ti}^{4+})\text{O}_4$, respectively (T, tetrahedral sites; M, octahedral sites). The solid solutions along the join Fe_3O_4 – Fe_2TiO_4 clearly involve not

only a cation substitution of Ti^{4+} for Fe^{3+} on the M sites, but also an electron exchange reaction between the T and M sites. In addition, this complexity is exacerbated by the well-known order–disorder phenomenon in the spinel structure due to variation of temperature (Liu and Prewitt 1990; O'Neill et al. 2003), pressure (Antao et al. 2005; Rozenberg et al. 2007) or composition (Wechsler et al. 1984; Diego Gatta et al. 2014). Further, the stoichiometry of the solid solutions along the join Fe_3O_4 – Fe_2TiO_4 is highly sensitive to the oxygen fugacity in their synthesizing experiments (Taylor 1964). Unfortunately, both the exact synthesizing temperature and oxygen fugacity and the detailed chemical compositions for the solid solutions used in Yamanaka et al. (2009 and 2013) are not available. More investigation on the solid solutions between magnetite and ulvöspinel is obviously necessary if one aims to understand the cause to the correlations between the K_T and chemical composition, as shown in Fig. 5.

Acknowledgments We thank two anonymous reviewers for their constructive comments on our manuscript. We also thank Dr. T. Tsuchiya for processing our manuscript. The in situ X-ray diffraction experiments were carried out at the National Synchrotron Light Source (NSLS), which is supported by the U.S. Department of Energy, Division of Materials Sciences and Division of Chemical Sciences under Contract No. DE-AC02-76CH00016. The operation of X17C is supported by COMPRES, the Consortium for Materials Properties Research in Earth Sciences. This work is financially supported by the Natural Science Foundation of China (Grant No. 41273072).

References

- Akimoto S, Syono Y (1967) High-pressure decomposition for some titanate spinels. *J Chem Phys* 47:1813–1817
- Andersen DJ, Lindsley DH (1988) Internally consistent solution models for Fe–Mg–Mn–Ti oxides: Fe–Ti oxides. *Am Mineral* 73:714–726
- Anderson DL, Anderson OL (1970) The bulk modulus–volume relationship for oxides. *J Geophys Res* 75:3494–3500
- Anderson OL, Nafe JE (1965) The bulk modulus–volume relationship for oxide compounds and related geophysical problems. *J Geophys Res* 70:3951–3963
- Angel RJ (2000) Equation of state. In: Hazen RM, Downs RT (eds) High-temperature and high-pressure crystal chemistry. *Reviews in Mineralogy and Geochemistry*, vol 41. Mineralogical Society of America, Chantilly, pp 35–60
- Antao SM, Hassan I, Crichton WA, Parise JB (2005) Effects of high pressure and high temperature on cation ordering in magnesioferrite, MgFe_2O_4 , using in situ synchrotron X-ray powder diffraction up to 1430 K and 6 GPa. *Am Mineral* 90:1500–1505
- Birch F (1947) Finite elastic strain of cubic crystals. *Phys Rev* 71:809–924
- Bosi F, Hälenius U, Skogby H (2008) Stoichiometry of synthetic ulvöspinel single crystals. *Am Mineral* 93:1312–1316
- Bosi F, Hälenius U, Skogby H (2009) Crystal chemistry of the magnetite–ulvöspinel series. *Am Mineral* 94:181–189
- Buddington AF, Lindsley DH (1964) Iron–titanium oxide minerals and synthetic equivalents. *J Petrol* 5:310–357

- Cameron EN (1971) Opaque minerals in certain lunar rocks from Apollo 12. *Proc Second Lunar Sci Conf* 1:193–206
- Chang L, Chen Z, Liu X, Wang H (2013) Expansivity and compressibility of wadeite-type $K_2Si_4O_9$ determined by in situ high T/P experiments, and their implication. *Phys Chem Mineral* 40:29–40
- Chopelas A, Hofmeister AM (1991) Vibrational spectroscopy of aluminate spinels at 1 atm and of $MgAl_2O_4$ to over 200 kbar. *Phys Chem Mineral* 18:279–293
- Diego Gatta G, Kantor I, Boffa Ballaran T, Dubrovinsky L, McCammon C (2007) Effect of non-hydrostatic conditions on the elastic behaviour of magnetite: an in situ single-crystal X-ray diffraction study. *Phys Chem Mineral* 34:627–635
- Diego Gatta G, Bosi F, McIntyre GJ, Hälenius U (2014) Static positional disorder in ulvöspinel: a single-crystal neutron diffraction study. *Am Mineral* 99:255–260
- Fei Y (1995) Thermal expansion. In: Ahrens TJ (eds) *Mineral physics and crystallography: a handbook of physical constants*. American Geophysical Union, Washington, DC, Shelf 2, pp 29–44
- Fleet ME (1981) The structure of magnetite. *Acta Crystallogr B* 37:917–920
- Fleet ME, Liu X, Shieh SR (2010) Structural change in lead fluorapatite at high pressure. *Phys Chem Mineral* 37:1–9
- Forster RH, Hall EO (1965) A neutron and X-ray diffraction study of ulvöspinel, Fe_2TiO_4 . *Acta Crystallogr* 18:859–862
- Haavik C, Stølen S, Fjellvåg H, Hanfland M, Häusermann D (2000) Equation of state of magnetite and its high-pressure modification: thermodynamics of the Fe-O system at high pressure. *Am Mineral* 85:514–523
- Hammersley J (1996) Fit2D report. Europe Synchrotron Radiation Facility, Grenoble, France
- He Q, Liu X, Hu X, Deng L, Chen Z, Li B, Fei Y (2012) Solid solutions between lead fluorapatite and lead fluorvanadate apatite: compressibility determined by using a diamond-anvil cell coupled with synchrotron X-ray diffraction. *Phys Chem Mineral* 39:219–226
- He Q, Liu X, Li B, Deng L, Chen Z, Liu X, Wang H (2013) Expansivity and compressibility of strontium and barium fluorapatite: significance of the M-site cations. *Phys Chem Mineral* 40:349–360
- Hofmeister AM, Mao HK (2001) Evaluation of shear moduli and other properties of silicates with the spinel structure from IR spectroscopy. *Am Mineral* 86:622–639
- Ishikawa Y, Sato S, Syono Y (1971) Neutron and magnetic studies of a single crystal of Fe_2TiO_4 . *J Phys Soc Jpn* 31:452–460
- Klotz S, Chervin JC, Munsch P, Le Marchand G (2009) Hydrostatic limits of 11 pressure transmitting media. *J Phys D Appl Phys* 42:075413
- Kyono A, Ahart M, Yamanaka T, Gramsch S, Mao HK, Hemley RJ (2011) High-pressure Raman spectroscopic studies of ulvöspinel Fe_2TiO_4 . *Am Mineral* 96:1193–1198
- Liebermann RC, Jackson I, Ringwood AE (1977) Elasticity and phase equilibria of spinel disproportionation reactions. *Geophys J R astr Soc* 50:553–586
- Lilova KI, Pearce CI, Gorski C, Rosso KM, Navrotsky A (2012) Thermodynamics of the magnetite-ulvöspinel (Fe_3O_4 – Fe_2TiO_4) solid solution. *Am Mineral* 97:1330–1338
- Liu X, Prewitt CT (1990) High-temperature X-ray diffraction study of Co_3O_4 : transition from normal to disordered spinel. *Phys Chem Mineral* 17:168–172
- Liu X, Shieh SR, Fleet ME, Akhmetov A (2008) High-pressure study on lead fluorapatite. *Am Mineral* 93:1581–1584
- Liu X, Shieh SR, Fleet ME, Zhang L (2009) Compressibility of a natural kyanite to 17.5 GPa. *Prog Nat Sci* 19:1281–1286
- Mao HK, Bell PM, Shaner JW, Steinberg DJ (1978) Specific volume measurements of Cu, Mo, Pt, and Au and calibration of ruby R1 fluorescence pressure gauge for 0.006 to 1 Mbar. *J Appl Phys* 49:3276–3283
- O'Neill HStC, Pownceby MI, Wall VJ (1988) Ilmenite-rutile-iron and ulvöspinel-ilmenite-iron equilibria and the thermochemistry of ilmenite ($FeTiO_3$) and ulvöspinel (Fe_2TiO_4). *Geochim Cosmochim Acta* 52:2065–2072
- O'Neill HStC, Redfern SAT, Kesson S, Short S (2003) An in situ neutron diffraction study of cation disordering in synthetic qandilite Mg_2TiO_4 at high temperatures. *Am Mineral* 88:860–865
- Ôno K, Chandler L, Ito A (1968) Mössbauer study of the ulvöspinel, Fe_2TiO_4 . *J Phys Soc Jpn* 25:174–176
- Reichmann HJ, Jacobsen SD (2004) High-pressure elasticity of a natural magnetite crystal. *Am Mineral* 89:1061–1066
- Rozenberg GK, Amiel Y, Xu WM, Pasternak MP, Jeanloz R, Hanfland M, Taylor RD (2007) Structural characterization of temperature- and pressure-induced inverse↔normal spinel transformation in magnetite. *Phys Rev B* 75:020102(R)
- Sedler IK, Feenstra A, Peters T (1994) An X-ray powder diffraction study of synthetic (Fe, Mn) $_2TiO_4$ spinel. *Eur J Mineral* 6:873–885
- Spencer K, Lindsley DH (1981) A solution model for coexisting iron-titanium oxides. *Am Mineral* 66:1189–1201
- Syono Y, Fukai Y, Ishikawa Y (1971) Anomalous elastic properties of Fe_2TiO_4 . *J Phys Soc Jpn* 31:471–476
- Taylor RW (1964) Phase equilibria in the system FeO – Fe_2O_3 – TiO_2 at 1300 °C. *Am Mineral* 49:1016–1030
- Tronche EJ, van Parker Kan M, de Vrse J, Wang Y, Sanehira T, Li J, Chen B, Gao L, Klemme S, McCammon CA, van Westrenen W (2010) The thermal equation of state $FeTiO_3$ ilmenite based on in situ X-ray diffraction at high pressures and temperatures. *Am Mineral* 95:1708–1716
- Wang Z, O'Neill HSC, Lazor P, Saxena SK (2002) High pressure Raman spectroscopic study of spinel $MgCr_2O_4$. *J Phys Chem Solids* 63:2057–2061
- Wang Z, Schiferl D, Zhao Y, O'Neill H St C (2003) High pressure Raman spectroscopy of spinel-type ferrite $ZnFe_2O_4$. *J Phys Chem Solids* 64:2517–2523
- Wang S, Liu X, Fei Y, He Q, Wang H (2012) In situ high-temperature powder X-ray diffraction study on the spinel solid solutions ($Mg_{1-x}Mn_x$) Cr_2O_4 . *Phys Chem Mineral* 39:189–198
- Wechsler BA, Prewitt CT (1984) Crystal structure of ilmenite ($FeTiO_3$) at high temperature and at high pressure. *Am Mineral* 69:176–185
- Wechsler BA, Lindsley DH, Prewitt CT (1984) Crystal structure and cation distribution in titanomagnetites ($Fe_{3-x}Ti_xO_4$). *Am Mineral* 69:754–770
- Wu Y, Wu X, Qin S (2012) Pressure-induced phase transition of Fe_2TiO_4 : X-ray diffraction and Mössbauer spectroscopy. *J Solid State Chem* 185:72–75
- Yamanaka T, Mine T, Asogawa S, Nakamoto Y (2009) Jahn-Teller transition of Fe_2TiO_4 observed by maximum entropy method at high pressure and low temperature. *Phys Rev B* 80:134120
- Yamanaka T, Kyono A, Nakamoto Y, Meng Y, Kharlamova S, Struzhkin VV, Mao HK (2013) High-pressure phase transitions of $Fe_{3-x}Ti_xO_4$ solid solution up to 60 GPa correlated with electronic spin transition. *Am Mineral* 98:736–744
- Yong W, Botis S, Shieh SR, Shi W, Withers AC (2012) Pressure-induced phase transition study of magnesiocromite ($MgCr_2O_4$) by Raman spectroscopy and X-ray diffraction. *Phys Earth Planet Inter* 196–197:75–82